17D.6 Objectively Identifying Transverse Cirrus Bands in Tropical Cyclones using a Convolutional Neural Network

John Mark Mayhall[*, 1, 2], Patrick Duran[2], Andrew White[1], Ryan Wade[1]
[1]University of Alabama in Huntsville
[2]NASA Marshall Space Flight Center, Huntsville, AL

*

1 INTRODUCTION

Transverse cirrus bands (TCBs) are a phenomenon that occurs in many mesoscale and synoptic weather systems, including tropical cyclones. TCBs are defined as "Bands of clouds oriented perpendicular to the flow in which they are embedded" (NWS) and can be associated with low static stability and high vertical wind shear in the upper-levels (Kawashima 2021), along with small Rossby numbers. TCBs in tropical cyclones are of particular interest due to their apparent occurrence and potential linkage to the tropical cyclone diurnal cycle (Dunion et al.), stronger tropical cyclones, and rapid intensification, where rapid intensification is an intensification rate of 30 knots or more in 24 hours (NHC). To fully understand TCBs and how they relate to tropical cyclones, they must be efficiently identified, which can be achieved through a machine-learning model. Miller et al. (2018) developed an image classification model that identified whether TCBs were present anywhere within a satellite image. However, this model does not provide information on the spatial structure of the bands and their location relative to a feature of interest, such as a tropical cyclone. This task is particularly suited for a U-Net model (Ronneberger et al.). While a CNN can be used to identify whether TCBs are in an image, a U-Net allows for the specific location of a TCB and the number of pixels a TCB makes up to be identified through the use of image segmentation.

U-Nets are a type of model that can be used to identify features present in a dataset by comparing manually identified features to features that are predicted using a training dataset, which is composed of arrays. U-Nets require an array to be reduced in size, which means the image is blurred and then increased in size back to the array's original size, which means an array must have a row and column length divisible by two for each layer used in the model. U-Nets also utilize a variety of methods to improve learning, such as dropping out certain memory nodes to force the model to utilize different methods of identification and normalizing the outputted data to create a normal distribution (O'Shea and Nash 2015). The condensed architecture of the U-Net model used in this study can be seen in Figure 1.

*Corresponding author address: John Mark Mayhall, Department of Atmospheric and Earth Science, NSSTC 3022, University of Alabama in Huntsville, 320 Sparkman Dr NW, Huntsville, AL 35805
Email: jmm0111@uah.edu

2 MODEL TRAINING AND METHODOLOGY

2.1 MODEL CREATION AND TRAINING

The first step of the U-Net model creation was the selection of which GOES-16 Advanced Baseline Imagery (ABI) channel or channels would be used to train the model and identify TCBs. After initial model testing, channels 13 (clean-IR) and 8 (upper-level water vapor) were chosen as they resulted in a model that produced accurate TCB areas with high confidence. These channels were chosen over visible and near-infrared channels, such as channel 4 (Cirrus Band), due to their ability to identify TCBs both at night and during the day. TCBs were manually identified, and the coordinates were saved to train the model. A total of 387 training cases were used, along with 130 verification cases that all came from 2018 Atlantic tropical cyclones, with images taken every three hours. The used tropical cyclones were identified based on the Statistical Hurricane Intensity Prediction Scheme (SHIPS) dataset and occurred within an area of the Atlantic defined by Figure 2. After the manually identified data was collected, the GOES-16 ABI files were downloaded from the National Oceanic and Atmospheric Administration's Amazon Web Services repository and converted to arrays along with the coordinate files, where the coordinate files became arrays of ones and zeroes to indicate the presence or absence of TCBs at a given pixel. The data for channels 13 and 8 were also scaled using Scikit-Learn's Standard Scaler to normalize the data. Missing data was assigned a large value much higher than the other values so the model would learn to ignore it. The U-Net was then trained until a minimum was reached in the validation loss function, which utilized a weighted binary cross-entropy function. The weighted binary cross entropy allowed for TCB areas to be weighted more than null areas and helped the model learn what a TCB is by preventing the model from ignoring all areas due to the overall greater size of null areas, which are areas without TCBs.

2.2 CREATION OF TRANSVERSE CIRRUS BAND STATISTICS

After the creation of the model, error statistics were performed to determine an ideal probability threshold that would minimize false positives while still identifying TCBs. The reason a probability threshold is needed is that the model outputs a percentage for each pixel, showing how confident the model is that the pixel is part of a TCB. The

binary Jaccard Score, which is the true positives divided by the sum of the true positives, false positives, and false negatives, was determined to be the best choice. The binary Jaccard Score maximizes the true area that is predicted correctly and is not affected by the large number of null pixels. The true arrays used for the error statistics were created by manual identification of TCBs in 2019 Atlantic tropical cyclones using the same criteria as the training and validation dataset, with 351 images being used. The Jaccard Score provided a probability threshold of 2% since the model tends to under-predict. An example of the model identifying TCBs using the Jaccard Score probability threshold can be seen in Figure 3, which clearly demonstrates the ability of the model to not only identify TCBs but also to identify them with high confidence. Figure 3 is only one example of the model, which performs similarly in other tropical cyclone imagery. A plot of the error statistics for all thresholds, including the binary Jaccard score, false-alarm-rate, and probability of detection is provided in Figure 4.

Two datasets were then used to relate the presence of TCBs to tropical cyclone structure and intensity. The HURDAT2 dataset (Landsea and Franklin 2013) was used to identify the tropical cyclone best track. Vertical wind shear over the 850-200 mb layer was obtained from the SHIPS dataset's SHDC and SDDC variables (DeMaria and Kaplan 1994). Both datasets were interpolated to hourly intervals to perform the statistics. Once the hourly data for all North Atlantic tropical cyclones from 2019 to 2022 was downloaded (a total of 6620 images), converted to arrays, and scaled, the model was run on the data. Using the TCB probabilities, statistics were generated, including a polar density map of TCB locations for the shear vector and radius, along with bar charts of the number of TCB pixels per time of day, rapid intensification status, and tropical cyclone intensities. The tropical cyclone intensity bar is based on the Saffir–Simpson scale, with tropical storms and depressions, category one and two hurricanes, and category three through five hurricanes grouped together. The bar charts were created by first sorting images and their associated amount of TCB pixels into bins. This was done multiple times to sort based on the time of day, intensity, and whether rapid intensification was occurring. Data for the bar charts were sorted into bins of TCB pixels based on the time of day, intensity, and whether rapid intensification was occurring. The total number of TCB pixels in each bin was then divided by the total number of all pixels (TCB plus non-TCB) in each bin to get a percentage.

3 RESULTS

3.1 TRANSVERSE CIRRUS BANDS RELATION TO SHEAR RELATIVE VECTORS AND RADIUS

After calculating the necessary TCB statistics, a polar density map of the number of TCB pixels per 50-kilometer radius and 0.5 degrees was created (Figure 5). From the figure, it is evident that TCBs occur most frequently in the downshear quadrants of tropical cyclones between 200 and 400 kilometers and less frequently close to a tropical cyclone's center, in the upshear quadrants, and at greater distances away from the tropical cyclone center. However, after normalizing the results to account for bin size increasing with radius, shown in Figure 6, it becomes apparent that TCBs occur in the upshear left quadrant as well.

3.2 TRANSVERSE CIRRUS BANDS RELATION TO TROPICAL CYCLONE STRENGTH AND THE DIURNAL CYCLE

Figure 7 shows the percentage of TCB pixels per image for different tropical cyclone strength intensities that are based on the Saffir–Simpson scale. Overall, category three and higher hurricanes, which have winds greater than 95 knots, had 18% of image pixels be TCBs, while category one and two hurricanes, which have winds of 64 to 95 knots, had a value of 17%, and tropical storms and depressions combined, which have winds less than 64 knots, had a value of 13%. Figure 8 shows the percentage of TCB pixels per image for a tropical cyclone's rapid intensification status. Overall, TCBs were more common in tropical cyclones undergoing rapid intensification than in storms not undergoing rapid intensification. Figure 9 compares the probability of TCBs in tropical cyclones at four different times of day using the percentage of TCB pixels per image. At times near noon local time, there was a relative minimum in TCB activity.

3.3 CONCLUSION

A U-Net CNN was trained to successfully identify TCBs in GOES-16 ABI imagery and was used to relate the presence of TCBs to tropical cyclone structure and intensity. TCBs occur more frequently in the downshear quadrants of a tropical cyclone along with the upshear left quadrant, in tropical cyclones with greater intensity, in tropical cyclones undergoing rapid intensification, and in the evening hours. In the future, statistical significance testing will be performed to confirm the statistical significance of the results.

4 REFERENCES

AWS, NOAA. AWS S3 Explorer. noaa-goes16.s3.amazonaws.com/index.html. Accessed 3/4/2024.

DeMaria, Mark, and John Kaplan. “A Statistical Hurricane Intensity Prediction Scheme (SHIPS) for the Atlantic Basin”. *Weather and Forecasting*, vol. 9, no. 2, June 1994, pp. 209–20. https://doi.org/10.1175/1520-0434(1994)009<0209:ASHIPS>2.0.CO;2.

Dunion, Jason P., et al. “The Tropical Cyclone Diurnal Cycle of Mature Hurricanes”. *Monthly Weather Review*, vol. 142, no. 10, Oct. 2014, pp. 3900–19. https://doi.org/10.1175/MWR-D-13-00191.1.

Kawashima, Masayuki. “A Numerical Study of Cirrus Bands and Low-Static-Stability Layers Associated with Tropical Cyclone Outflow”. *Journal of the Atmospheric Sciences*, vol. 78, no. 11, Nov. 2021, pp. 3691–716. https://doi.org/10.1175/JAS-D-21-0047.1.

Knox, John A., et al. “Transverse cirrus bands in weather systems: a grand tour of an enduring enigma”. *Weather*, vol. 65, no. 2, 2010, pp. 35–41. https://doi.org/10.1002/wea.417.

Landsea, Christopher W., and James L. Franklin. “Atlantic Hurricane Database Uncertainty and Presentation of a New Database Format”. *Monthly Weather Review*, vol. 141, no. 10, Oct. 2013, pp. 3576–92. https://doi.org/10.1175/MWR-D-12-00254.1.

Lenz, A., et al. “Convectively Induced Transverse Band Signatures in Satellite Imagery”. *Weather and Forecasting*, vol. 24, no. 5, Oct. 2009, pp. 1362–73. https://doi.org/10.1175/2009WAF2222285.1.

Miller, Jeffrey, et al. “Detection of transverse cirrus bands in satellite imagery using deep learning”. *Computers & Geosciences*, vol. 118, Sept. 2018, pp. 79–85. https://doi.org/10.1016/j.cageo.2018.05.012.

NHC, NOAA. Glossary of NHC Terms. www.nhc.noaa.gov/aboutgloss.shtml#r. Accessed 3/4/2024.

NWS, NOAA. NOAA’s National Weather Service - Glossary. forecast.weather.gov/glossary.php?word=transverse%20bands. Accessed 3/4/2024.

O’Shea, Keiron, and Ryan Nash. “An Introduction to Convolutional Neural Networks”. Nov. 2015. https://doi.org/doi.org/10.48550/arXiv.1511.08458.

Ronneberger, Olaf, et al. “U-Net: Convolutional Networks for Biomedical Image Segmentation”. May 2015, arXiv:1505.04597 [cs]. arxiv.org/abs/1505.04597. Accessed 22/4/2024.

5 Figures

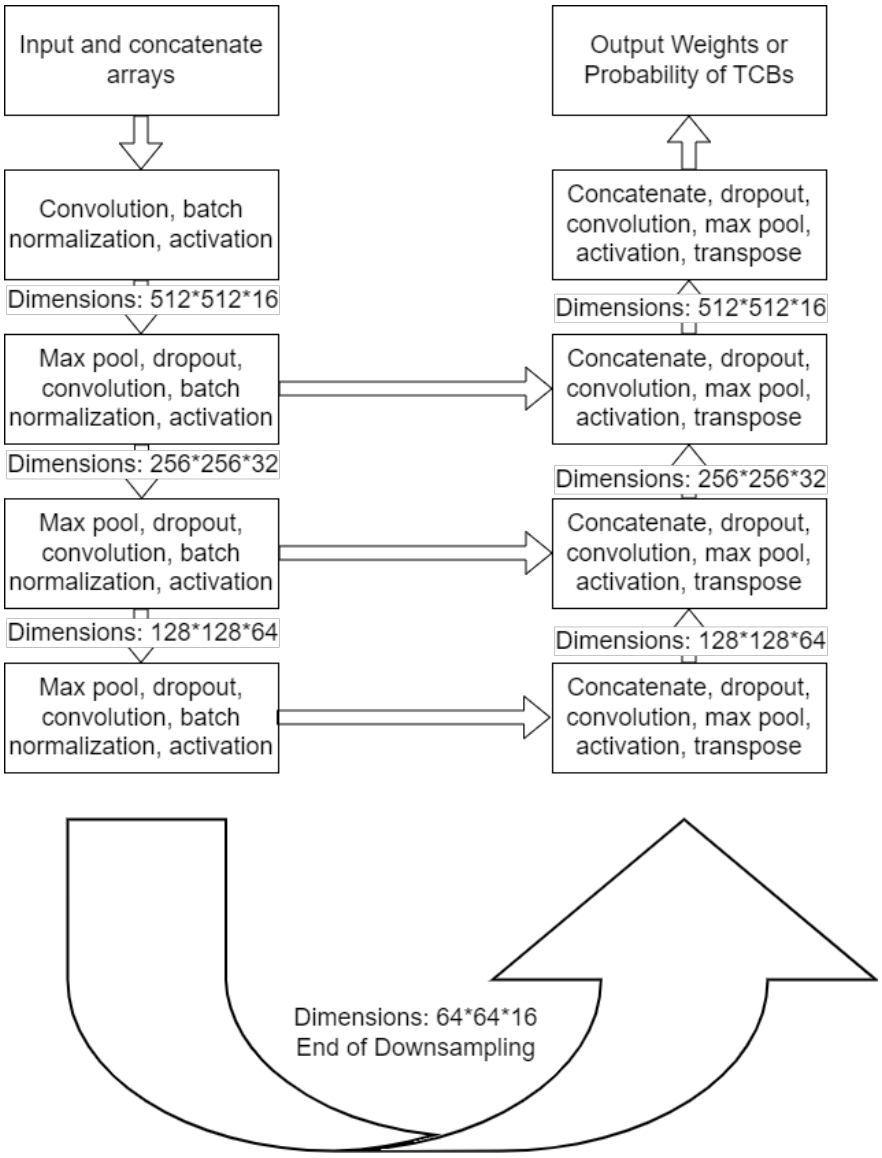


Figure 1: The U-Net CNN used in this study. The model has three layers and utilizes two inputs. The model also utilizes the dropout, max pooling, and batch normalization methods to improve model learning and confidence. The basic flow of the model is as follows. The ABI channel 13 and channel 8 arrays are inputted at the top of the diagram. The two arrays are then concatenated together to make one array. After that, the array is halved in size for each convolution, with an activation, batch normalization, max pooling, and dropout function being used each time except for the first convolution, which does not have a dropout or max pooling function. After the array is reduced to a 64 by 64 array from its initial size of 512 by 512, the U-net portion of the CNN begins. The same general process is applied except that the convolution function is replaced with a 2D convolution function. The array is then increased in size back to its original 512 by 512 dimensions.

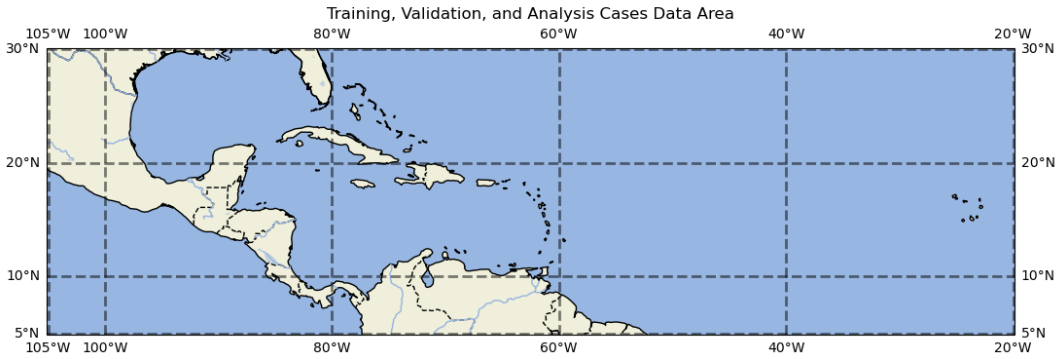


Figure 2: Area of interest used in the analysis. The area is bound by $5^{\circ}N$ and $30^{\circ}N$ latitude, along with $20^{\circ}W$ and $105^{\circ}W$ longitude.

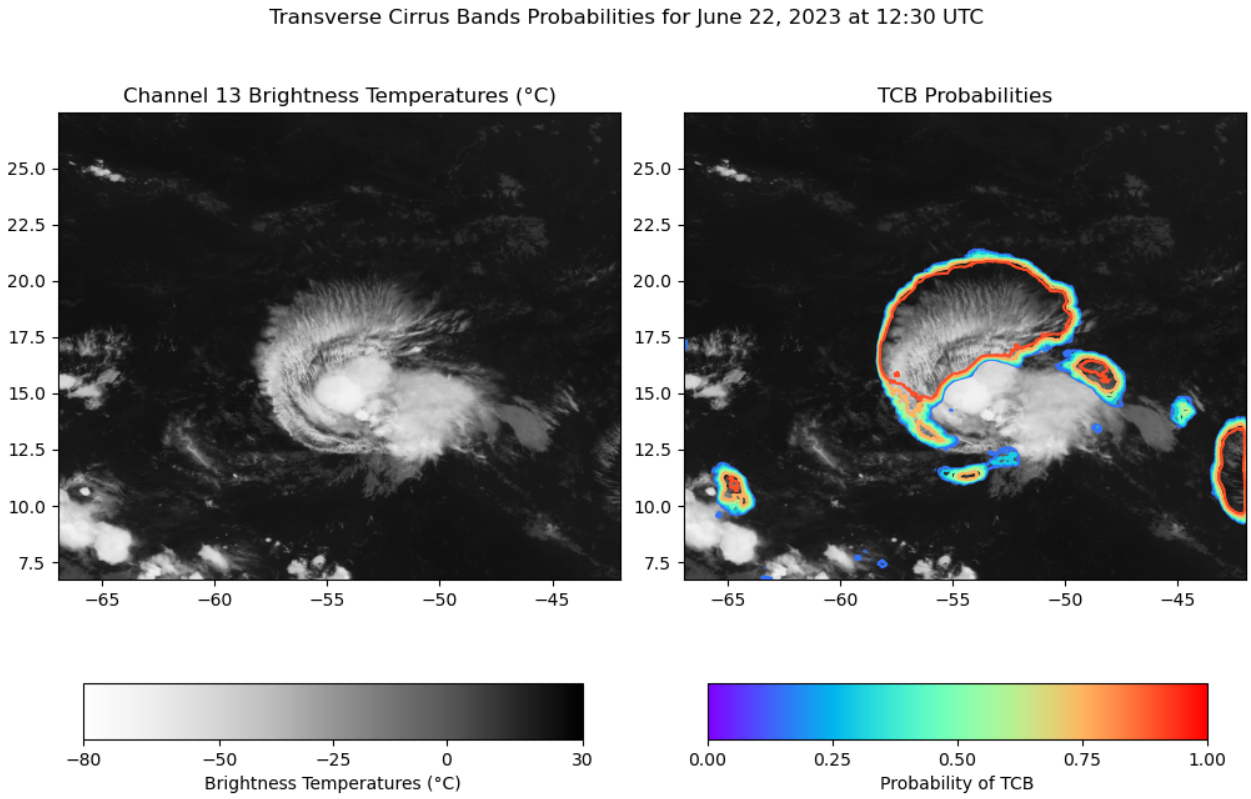


Figure 3: An example of the model used in the analysis. The left panel shows GOES-16 ABI Channel 13 brightness temperatures (degrees Celsius) in tropical cyclone Bret (AL022023), and the right panel is the same image with the probabilities of transverse bands at each pixel depicted in colored contours.

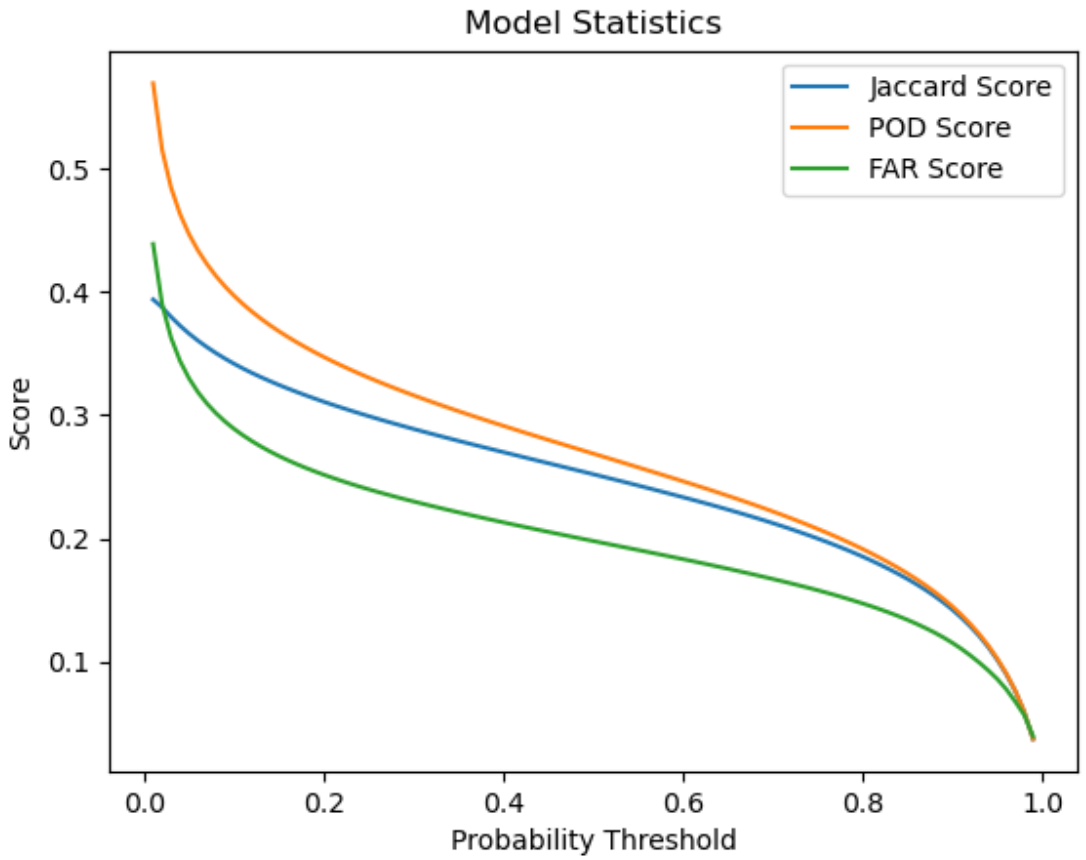


Figure 4: Error statistic scores plotted against cutoff thresholds. Note that the score does not change much until higher thresholds are reached due to the high gradient usually present in the model's predictions.

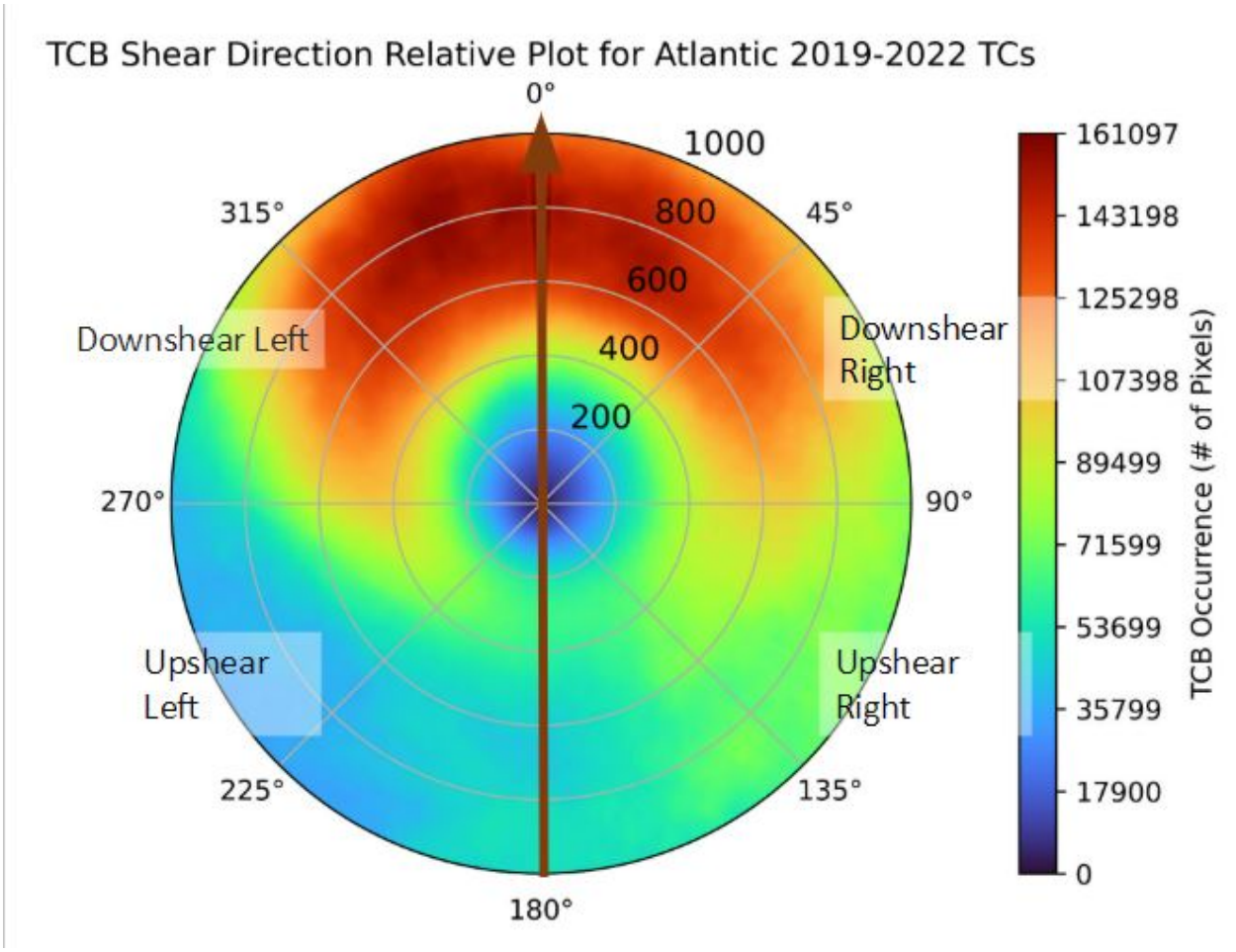


Figure 5: Storm-centered plot of the number of GOES-16 ABI pixels that contain TCBs at a given radius and shear relative azimuth. Zero degrees is downshear, 180 degrees is upshear, 90 degrees is right of shear, and 270 degrees is left of shear. Range rings are plotted every 200 km out to 1000 km.

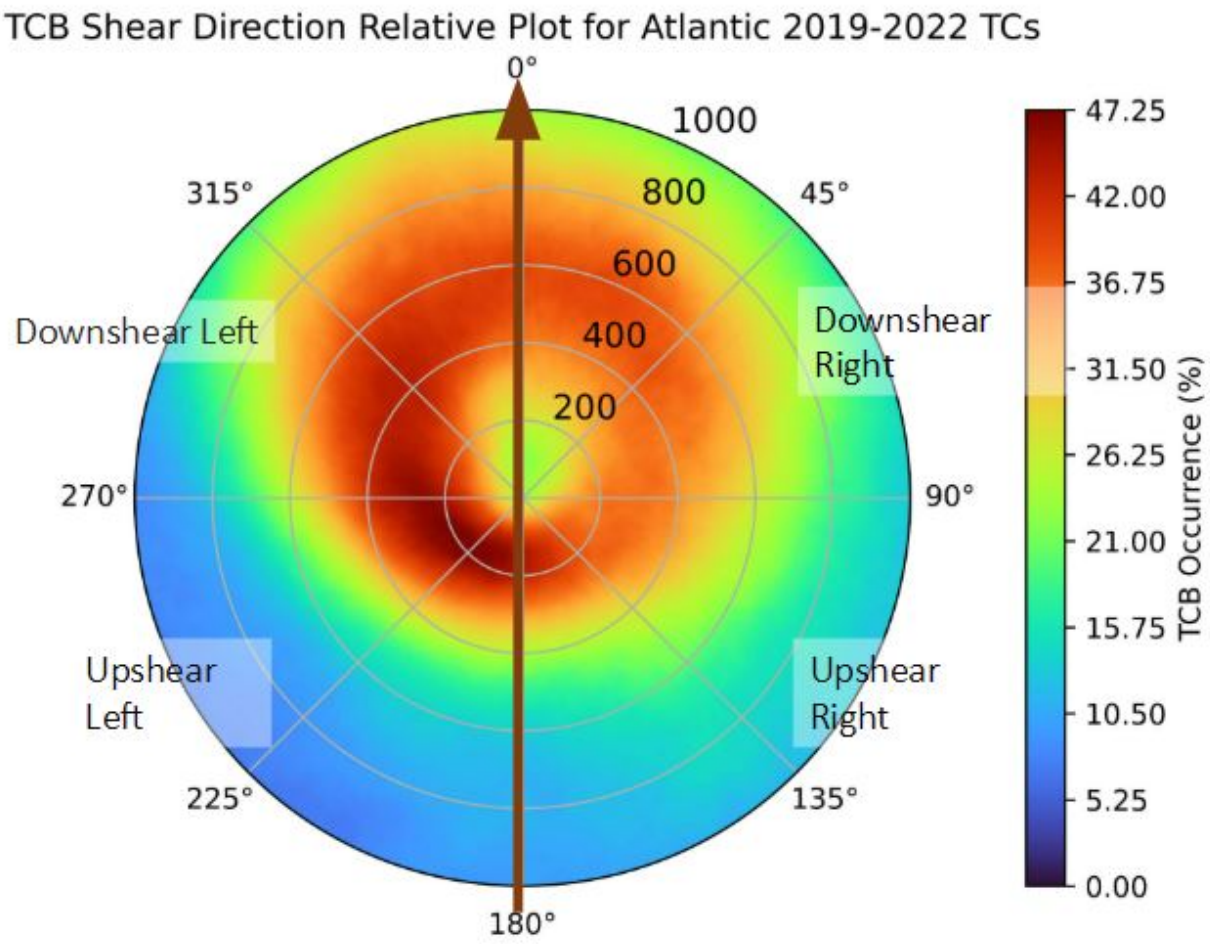


Figure 6: Storm-centered plot of the number of GOES-16 tropical cyclone images that contain TCBs at a given radius and shear relative azimuth, where the bins of the plot have been normalized by radius. Zero degrees is downshear, 180 degrees is upshear, 90 degrees is right of shear, and 270 degrees is left of shear. Range rings are plotted every 200 km out to 1000 km.

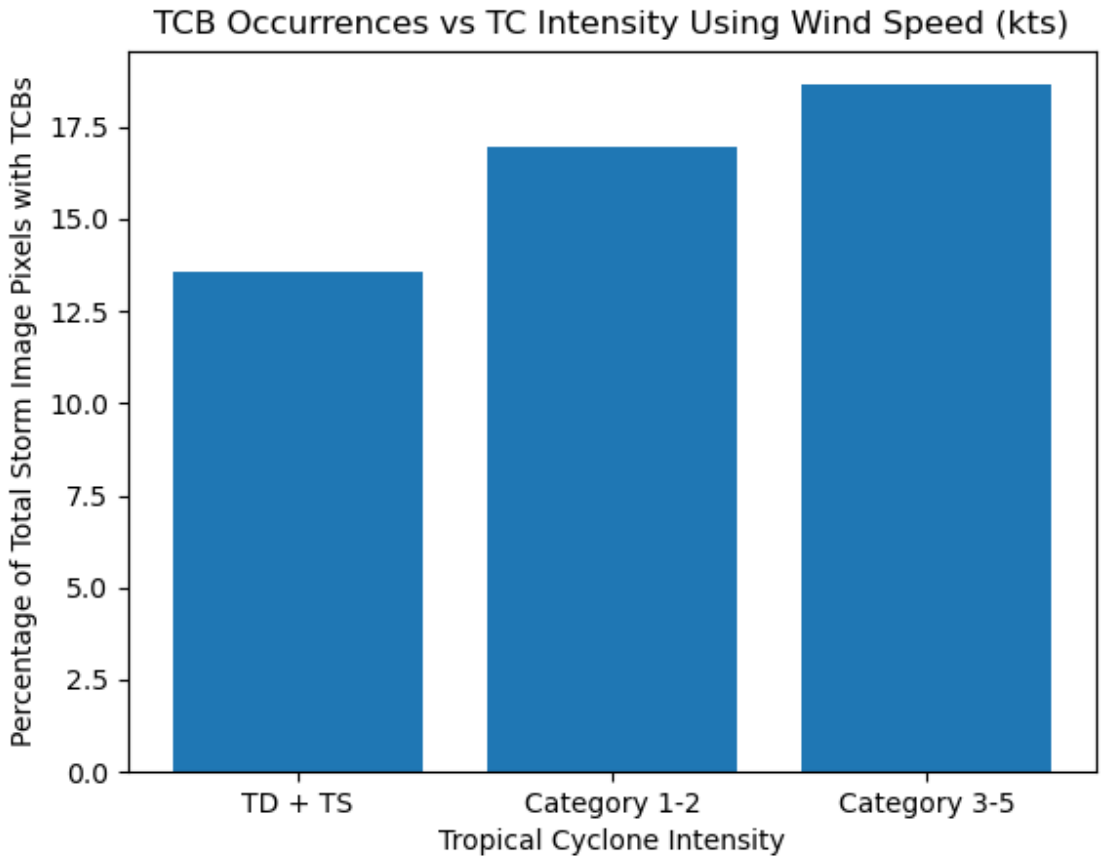


Figure 7: The percentage of pixels in an image that are TCBs for three different intensity bins. The y-axis shows the percentage of TCB pixels while the x-axis shows the tropical cyclone intensity, which is either a tropical depression or storm, category 1 and 2 hurricanes, or category 3 through 5 hurricanes.

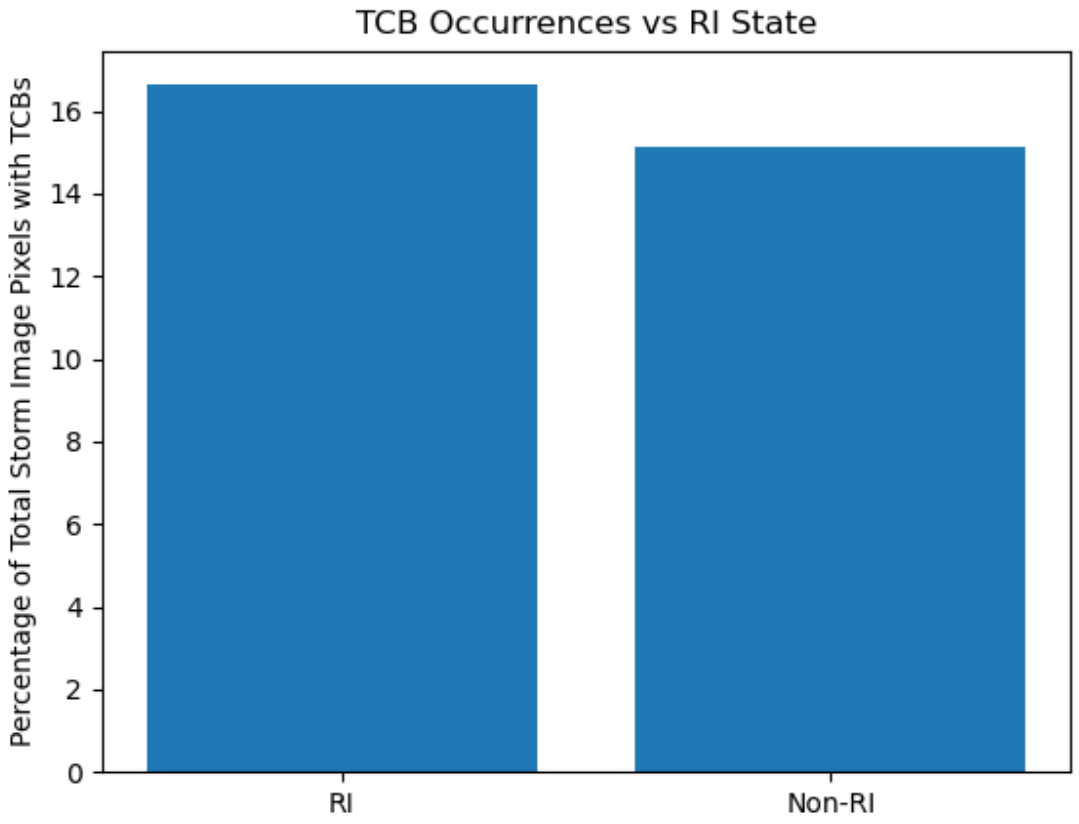


Figure 8: The percentages of pixels in an image that are TCBs for tropical cyclones undergoing rapid intensification and for tropical cyclones not undergoing rapid intensification. The y-axis shows the percentage of TCB pixels, while the x-axis shows rapid intensification and non-rapid intensification.

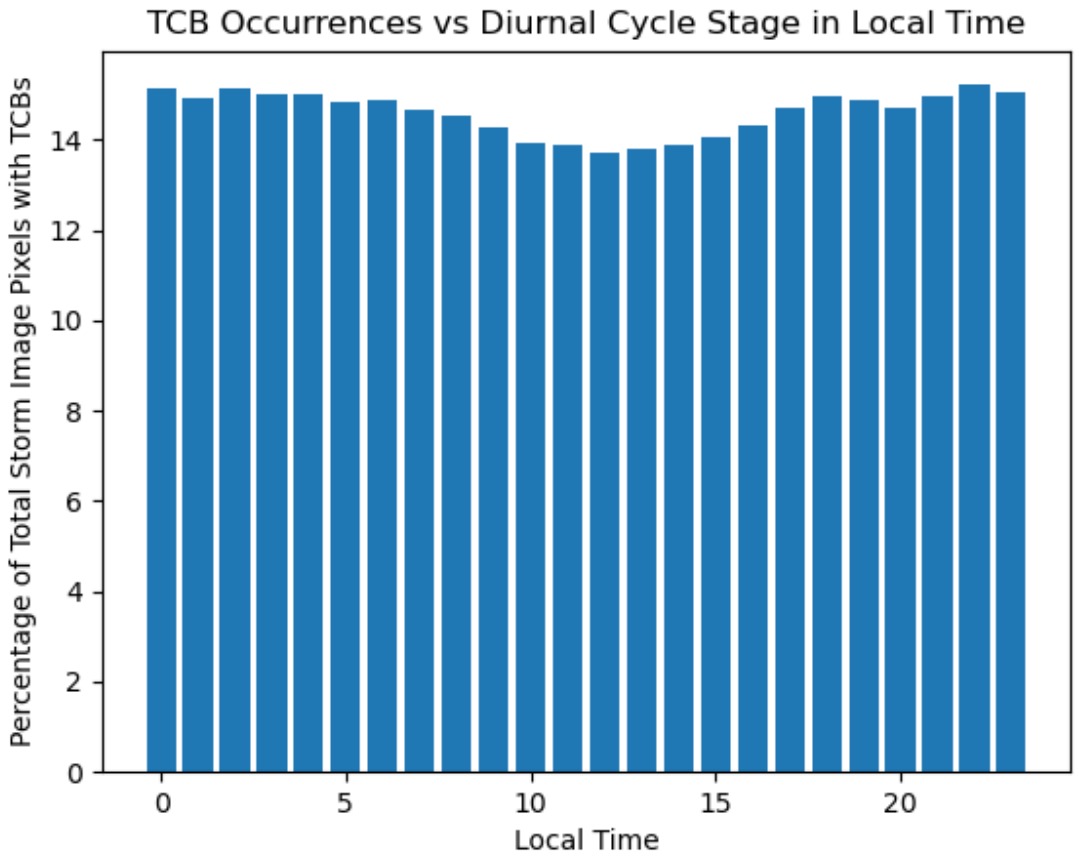


Figure 9: The percentages of pixels in an image that are TCBs binned by the hourly local time. Local time is shown on the x-axis, and the percentage is shown on the y-axis.